AAEC/E493

AAEC/E493

(3)

AUSTRALIAN ATOMIC ENERGY COMMISSION

RESEARCH ESTABLISHMENT

LUCAS HEIGHTS

ACOUSTIC EMISSION AND FAILURE PREDICTION FOR PRESSURISATION EXPERIMENTS ON HELICOPTER AIR BOTTLES

by

K.R. BROWN
R.W. HARRIS

November 1980

ISBN 0 642 59693 X

AUSTRALIAN ATOMIC ENERGY COMMISSION
RESEARCH ESTABLISHMENT
LUCAS HEIGHTS

ACOUSTIC EMISSION AND FAILURE PREDICTION FOR PRESSURISATION EXPERIMENTS ON HELICOPTER AIR BOTTLES

by

K.R. BROWN
R.W. HARRIS

ABSTRACT

Two spherical high pressure bottles of high-tensile steel were pressurised to destruction to evaluate acoustic emission monitoring as a non-destructive test on similar bottles. One bottle was tested with an artificially introduced defect of sufficient size to reduce the failure pressure to the proof-test pressure; the other contained no flaws. In neither bottle was sufficient acoustic emission detected to enable monitoring to be of value for non-destructive testing.

National Library of Australia card number and ISBN 0 642 59693 X

The following descriptors have been selected from the INIS Thesaurus to describe the subject content of this report for information retrieval purposes. For further details please refer to IAEA-INIS-12 (INIS: Manual for Indexing) and IAEA-INIS-13 (INIS: Thesaurus) published in Vienna by the International Atomic Energy Agency.

ACOUSTIC EMISSION TESTING; GAS CYLINDERS; STEELS; FAILURES

CONTENTS

1. INTRODUCTION

The Aircraft Maintenance and Repair Branch of the Department of Defence (Navy) has investigated the possibility of using acoustic emission to warn of the presence of defects in high pressure air bottles used on helicopters. These bottles are 320 mm diameter spheres of 3.25 mm wall thickness high tensile steel. The sphere is formed in two halves and joined by an equatorial weld. These vessels are designed for a maximum service pressure of 23 MPa (3300 psi) and proof-tested at 34 MPa (4950 psi). The vessels are made of 3 per cent chromium-molybdenum steel, heat-treated to achieve an ultimate tensile strength of 1275 MPa (185 ksi) which corresponds to a nominal burst pressure of 52 MPa (7500 psi). Because of the danger associated with the catastrophic failure of one of these bottles, and because of the difficulties in applying non-destructive tests to them, the life of the bottle is limited to ten years during operation in the temperature range -40°C to +90°C; a log book is maintained on each bottle.

This report describes a study of the possibility of using acoustic emission techniques during proof testing to confirm the safety of defect-free vessels, and to extend their service life, and a study of the prediction of failure.

Two bottles (Serial Nos. SD877 and SD853) were provided by the RAN for acoustic emission testing during inflation; the first is referred to as bottle 1 and the second as bottle 2. These bottles had been removed from service after 10 years.

2. EXPERIMENTAL INVESTIGATION

The welds on both bottles were examined by X- and gamma-radiography but no defects were discovered. Strain gauges were then attached to bottle 1 in the positions indicated in Figure 1. The strain gauge data and pressure instrumentation calibration are detailed in Appendix A. A single Dunegan acoustic emission sensor having a nominal resonance frequency of approximately 160 kHz was attached to the vessel which was then filled with a water and soluble oil mixture at ambient temperature (approximately 20°C), placed in a bunker, and pressurised with oil using a Dynapac hand-operated hydraulic pump. The bottle was pressurised to its proof-test pressure (34 MPa, 4950 psi); the pressure was then reduced to zero twice, before pressurisation was continued

to failure. All pressures were monitored with a calibrated dial gauge. During the three pressurisation tests, strain gauge and acoustic emission transducer outputs were recorded. Failure was catastrophic, despite the use of water as the pressurisation medium instead of air, which meant that a safety bunker is necessary for tests of this type.

During pressurisation of bottle 1, bottle 2 was placed in the same bunker, beside the pressurised vessel, with dummy strain gauges attached for temperature compensation; this process was reversed during the pressurisation of bottle 2. After failure, sections were cut from the bottle and flattened for tensile test specimens. These were used to determine the ultimate tensile strength, approximate yield strength and the elongation of the bottle material.

Using the failure stress data from bottle 1, fracture mechanics calculations were made to determine the size of defect necessary to reduce the failure pressure to the proof-test pressure. The length of an appropriate defect which penetrated approximately 50 per cent of the bottle wall thickness was then calculated by the methods outlined below; an artificial defect of these dimensions was machined in the bottle at the position shown in Figure 1(a). The defect profile is shown in Figure 1(b). Strain gauges were attached to the bottle at approximately 20 mm from each end of the machined defect and at positions on the bottle well away from the defect. The acoustic emission transducer was attached and the bottle filled and pressurised as described above but with the first two pressure cycles limited to 10 MPa (1450 psi). For this test, a pressure transducer connected to a chart recorder was used in addition to the dial pressure gauge.

3. ACOUSTIC EMISSION TEST RESULTS

Occasional acoustic emission bursts were detected during the three pressurisations of bottle 1. The Kaiser effect was observed; that is, during subsequent pressurisations no emission was detected until after the maximum pressure of the previous pressurisation was exceeded. The fact that some emission was observed during the initial inflation at pressures less than the service pressure indicates that some slight degree of 'acoustic recovery' may have been operative; however, it is more likely that these emissions originated in pressure fittings, e.g. the attached pressure tubing or the supports of the bottle. During the final pressurisation, the acoustic

activity was observed to rise with increasing pressure. However, no significant increase that could be construed as impending failure was detected until less than 10 seconds before failure. In fact, the pump operator was aware of impending failure before the acoustic emission warning as the pump loading became much 'softer' during the final few seconds.

It was thought that if a defect was present such that failure would occur at a lower pressure, local yielding in the tip of the defect could give enhanced acoustic emission earlier than was observed in the unflawed bottle. Consequently, an artificial defect was machined in the second bottle such that the failure pressure would be reduced to approximately the proof-test pressure; the bottle was then tested to failure. This bottle was pressurised to 10 MPa and deflated twice before the final pressurisation to failure. Occasional acoustic emission was detected during the first and last pressurisations at pressures exceeding 10 MPa. Again, no significant increase in acoustic emission activity was observed until several seconds before failure.

4. FAILURE PREDICTION

The failure pressure of the bottle in the presence of through-wall flaws of length 2c was calculated by the methods of Folias [1965] for thin-walled pressurised spheres. The hoop stress at failure, σ_F, is given by the equation:

$$\sigma_F = \frac{2\sigma}{\pi I} \cos^{-1}\left[\exp\left(\frac{-\pi K^2}{8\sigma^2 c}\right)\right] \qquad (1)$$

in which

$$I = 1 + \frac{3\pi\lambda^2}{64} \qquad (2)$$

$$\lambda^2 = \frac{c^2}{Rt}\left[12(1-\nu^2)\right]^{1/2} \qquad (3)$$

where σ = the flow stress of the material, R = the vessel radius, ν = Poisson's ratio, t = the wall thickness, and K = the material fracture toughness. Equation (2) may be simplified to

$$I = 1 + 0.96 \frac{c^2}{Rt} \tag{4}$$

For ductile materials in which the fracture toughness K becomes very large, the inverse cosine expression approaches $\pi/2$, and

$$\sigma_F = \frac{\sigma}{I} \tag{5}$$

The Folias relationships for through-wall flaws may be extended to partial thickness flaws using the methods of Duffy et al. [1969]. The failure stress for a partial thickness flaw is related to that of a through-thickness flaw of the same length by

$$\frac{\sigma_H}{\sigma_c} = \frac{A_o - A}{A_o - A\left(\frac{\sigma^*}{\sigma_c}\right)}$$

where σ_c is the failure stress for an unflawed tube, σ^* is the failure stress for a tube containing a through-wall defect of the same length as the surface defect, $A_o = 2Ct$, i.e. the area of the through-wall defect, and A is the area of the partial thickness defect.

The flow stress used in the Folias equation was determined from the yield stress and the ultimate tensile strength determined from fragments of bottle 1. However, the ultimate tensile strength yield stress could also be determined from the burst pressure and the pressure at which plastic strain was first detected on strain gauges attached to bottle 1. These values are in good agreement (Table 1).

The results indicate that a machined defect half way through the wall thickness and approximately 50 mm in length should reduce the failure pressure to the proof-test pressure. However, these predictions were markedly dependent on the value of the fracture toughness, K, selected for the material and the fragments of the material were of insufficient size to enable a determination to be made experimentally. Initially, a value of 135 MPa $m^{\frac{1}{2}}$ (120 ksi $\sqrt{in}$) was selected as appropriate for steels of this composition (Table 2); however, the machined defect was considerably blunter than the fatigue cracks typically used for the determination of the fracture toughness data. Consequently, a higher value of the fracture toughness would be expected, for the material is more resistant to blunt than sharp defects. Additionally, since the bottle wall thickness is insufficient to develop plane strain conditions during failure in a material of this strength and toughness,

the effective fracture toughness would again be higher. Such uncertainties make accurate failure prediction difficult but they could be reduced after tests on one flawed bottle; further prediction would then be much more accurate.

The results of these predictions are shown graphically in Figure 2 for both partial thickness and through-wall flaws for several assumed values of the fracture toughness K. The actual burst pressure of the flawed bottle is also shown. It can be seen that for a fracture toughness of 135 MPa $m^{\frac{1}{2}}$, the predicted failure stress is approximately 20 per cent low.

The hoop stress at failure in the vessel wall was also determined from the strain gauge output via the relationship

$$\sigma = \frac{E}{1-\nu} \cdot \varepsilon$$

where E is the Young's modulus taken as 2×10^5 MPa, ν is Poisson's ratio, and ε is the strain indicated by a uni-axial strain gauge on a bi-axially stressed surface.

The stresses at failure were calculated from the maximum strain gauge output recorded before bursting and these are expressed as equivalent pressures in Table 1. It can be seen that a very satisfactory agreement was obtained between this type of failure pressure and that determined from the indicated pressure at failure.

5. FAILURE MODES

Even though hydraulic pressurisation was used, both bottles failed catastrophically. Once the fracture had been initiated, it propagated in two directions from the initiation point, and almost completely encircled the bottle allowing it to hinge open (Figures 3 to 6).

In bottle 1, the fracture initiation point was adjacent to the nozzle weld; however, this was not associated with any defect in the weld. It is most probable that fracture started at this point owing to the restraint from the relatively rigid nozzle, which created local high stresses in the vicinity of the penetration. Failure in bottle 2 started at the machined defect and propagated into the full thickness of the material. No involvement of the

circumferential weld was noted and the fracture was not deflected when it intersected the weld; this would suggest satisfactory weld quality and structure.

During propagation and initiation, the fractures in both bottles were of the shear type and intersected the wall at approximately 45°. Under high magnification, the fracture face (Figure 7) appeared typical of ductile failures. There was no evidence of brittle cleavage failure; however, the centre of the steel plate had large numbers of inclusions which allowed separation to form large ductile dimples on the fracture face. The number of these inclusions is perhaps surprising for a steel of this quality and type; however, their presence clearly has not reduced the fracture energy or the strength of the bottles.

6. DISCUSSION

The failure of acoustic emission to give significant warning of the failure of the bottles may be taken as confirmation of Birchon's hypothesis, i.e. "because it was not heard it does not mean it did not happen" [Birchon 1976]. At ambient temperature, the material from which the bottles are made is not 'noisy' in an acoustic emission sense. Birchon found that crack growth in materials such as the tough steels used for many pressure vessels can be very difficult to detect. The failures encountered in bottles 1 and 2 were entirely ductile and their initiation was quiet. It is conceivable that useful warnings of impending failure might be obtained during proof-testing at temperatures below the material's nil ductility transition temperature; however, this has not been tried experimentally, nor has this temperature been determined.

In many steels of this type, significant acoustic emission at ambient temperature occurs only immediately before and during yield; once plastic flow is under way, acoustic emission diminishes rapidly until the very final phases of the fracture of the specimen. In uni-axial tensile test specimens taken from the bottle remains, yield occurred at approximately 90 per cent of the ultimate tensile strength. No plasticity was detected before failure in the bottle containing the artifical defect by strain gauges mounted 20 mm in front of the defect tips. Consequently, no large-scale plastic deformation of the bottle preceded failure. It is probable that the lack of significant warning of crack initiation occurred because crack nucleation and growth

followed closely after the yield stress had been reached.

7. ACKNOWLEDGEMENTS

We are indebted to the staff of the AAEC Inspection Department who set up and carried out the pressurisation. Thanks are due particularly to Mr E. Noon for the strain gauge measurements and Mr B. Zybenko for assistance with the experimental program.

8. REFERENCES

Birchon, D. [1976] - The Potential of Acoustic Emission in NDT. Br. J. Non-Destr. Test., 18(3)66.

Duffy, A.R., Eiber, R.J. and Maxey, W.A. [1969] - Recent Work on Flaw Behaviour in Pressure Vessels. Symp. on Fracture Toughness Concepts, UKAEA, Harwell, April.

Folias, E.S. [1965] - Finite Line Crack in a Pressurised Spherical Shell. Int. J. Fract. Mech., 1(1)20.

TABLE 1
YIELD AND BURST PRESSURES FOR BOTTLES

	Yield Pressure (MPa)			Burst Pressure (MPa)		
	A	B	C	A	B	C
Bottle 1	44.5	45.3	46.6	47.2	50.9	*
Bottle 2	-	-	-	33.6	-	33.7

A. Measured directly by calibrated pressure gauge (bottle 1) or transducer (bottle 2) - most accurate.

B. Calculated from uni-axial tensile data from fragments of bottle 1 only. Yield data inaccurate owing to curvature of test specimen. The hoop stress $\sigma = PR/2t$ where R is the bottle radius and t the wall thickness.

C. Calculated from uni-axial strain gauge data:

$$\sigma = \frac{E}{1-\nu} \cdot \varepsilon$$

where E is Young's modulus (2×10^5 MPa), ν is Poisson's ratio, (0.33), σ is the hoop stress and ε is the indicated strain.

* elastic and plastic strain.

TABLE 2
APPROXIMATE SPARK ANALYSIS OF BOTTLE 1

C	Mn	Cr	Mo	Cu	Si	Ni	V
				%			
-	1.0	2-4	0.2	0.1	0.6	<0.2	<0.1

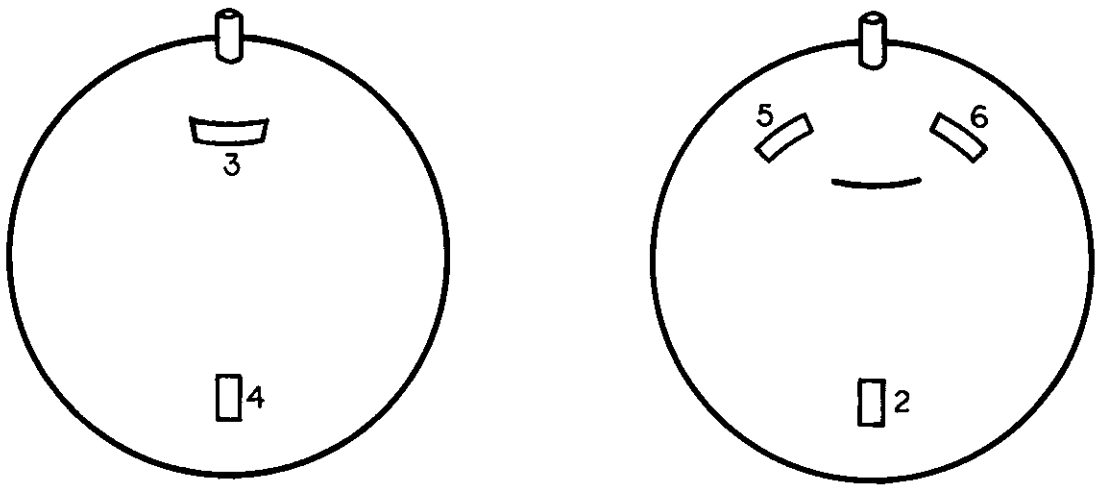

BOTTLE 1 **BOTTLE 2**

(a) Locations of defect and strain gauges

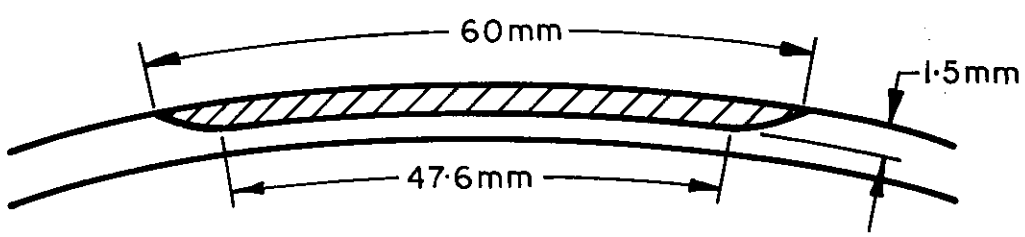

(b) Artificial defect profile. Effective length = 54 mm

FIGURE 1. DETAILS OF STRAIN GAUGES AND DEFECTS

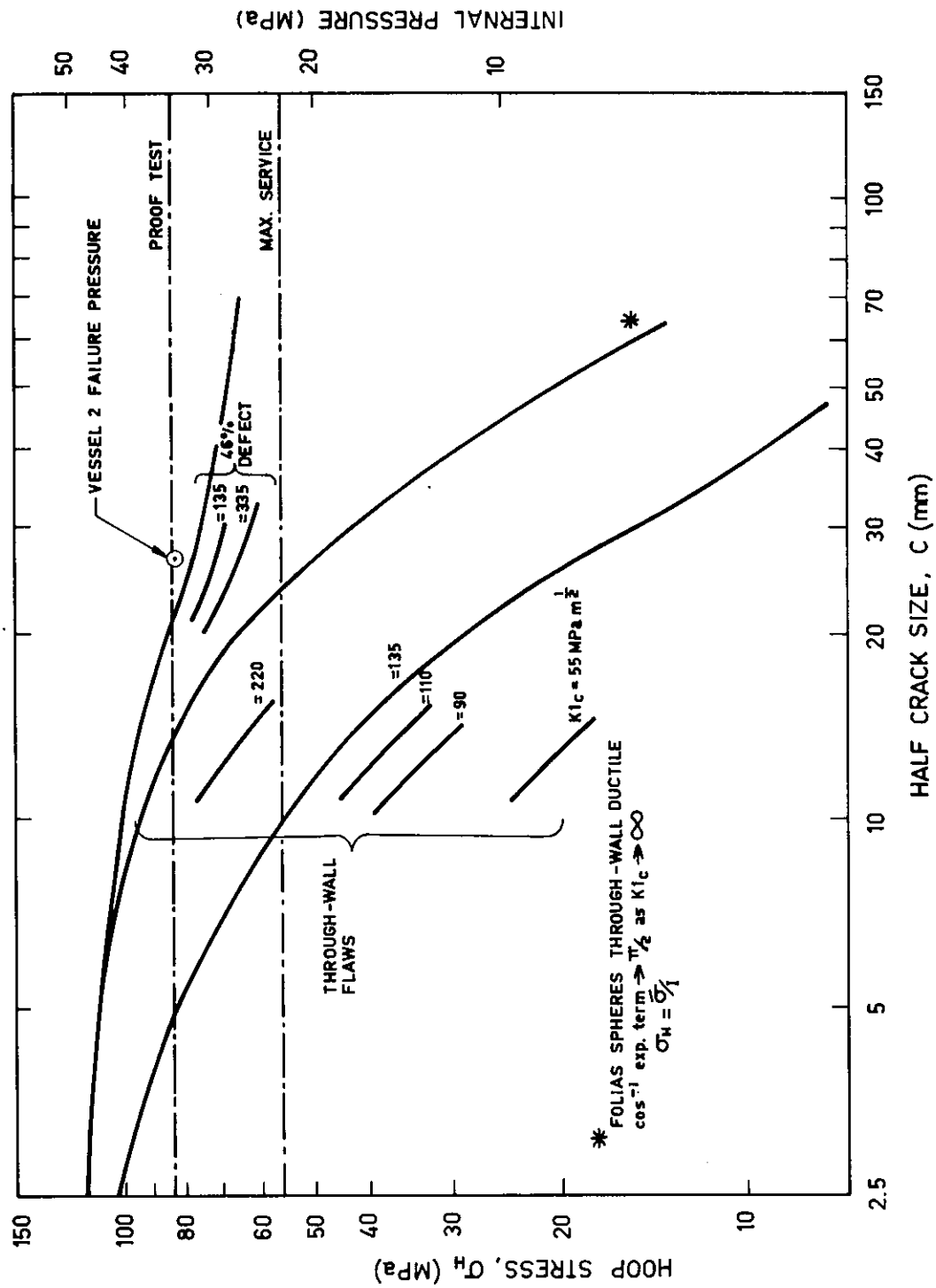

FIGURE 2. FAILURE STRESS VERSUS CRACK SIZE FOR THROUGH-WALL AND PARTIAL THICKNESS DEFECTS. THE SOLUTIONS OF THE FOLIAS EQUATIONS ARE SHOWN FOR VARIOUS INDICATED VALUES OF MATERIAL FRACTURE TOUGHNESS

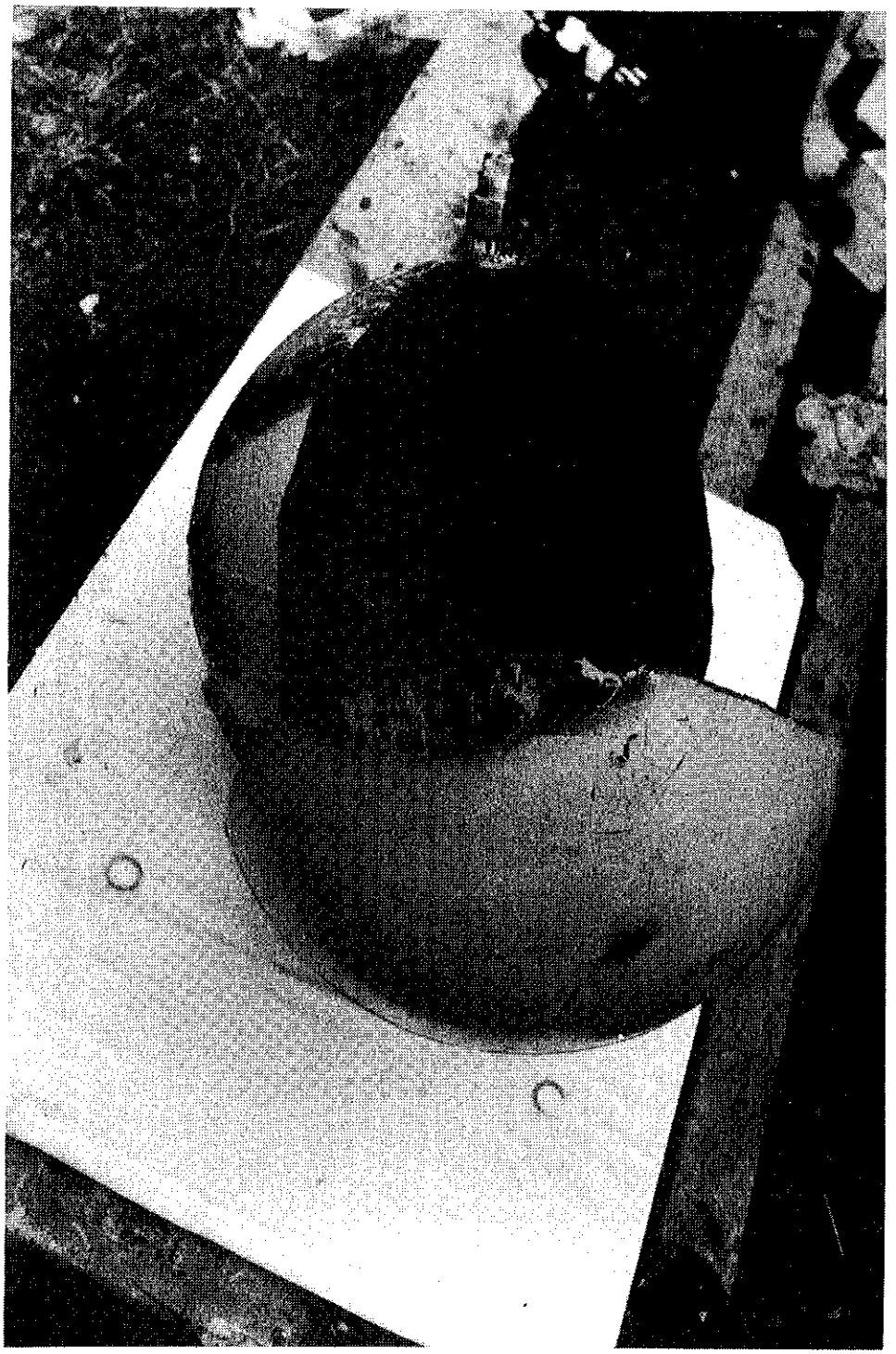

FIGURE 3. BOTTLE 1 AFTER PRESSURISATION TO FAILURE

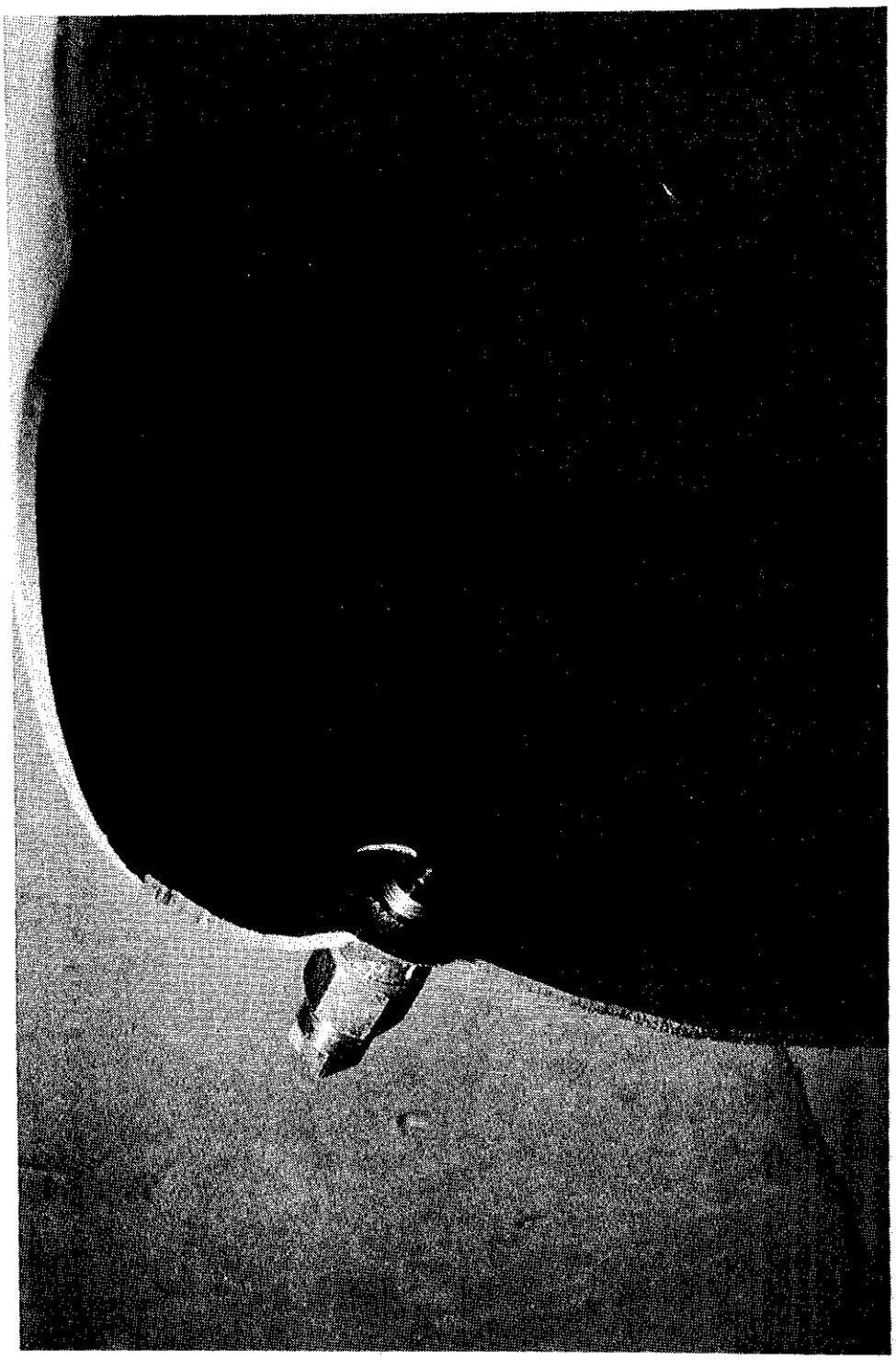

FIGURE 4. FAILURE INITIATION POINT ADJACENT TO THE NOZZLE ON BOTTLE 1

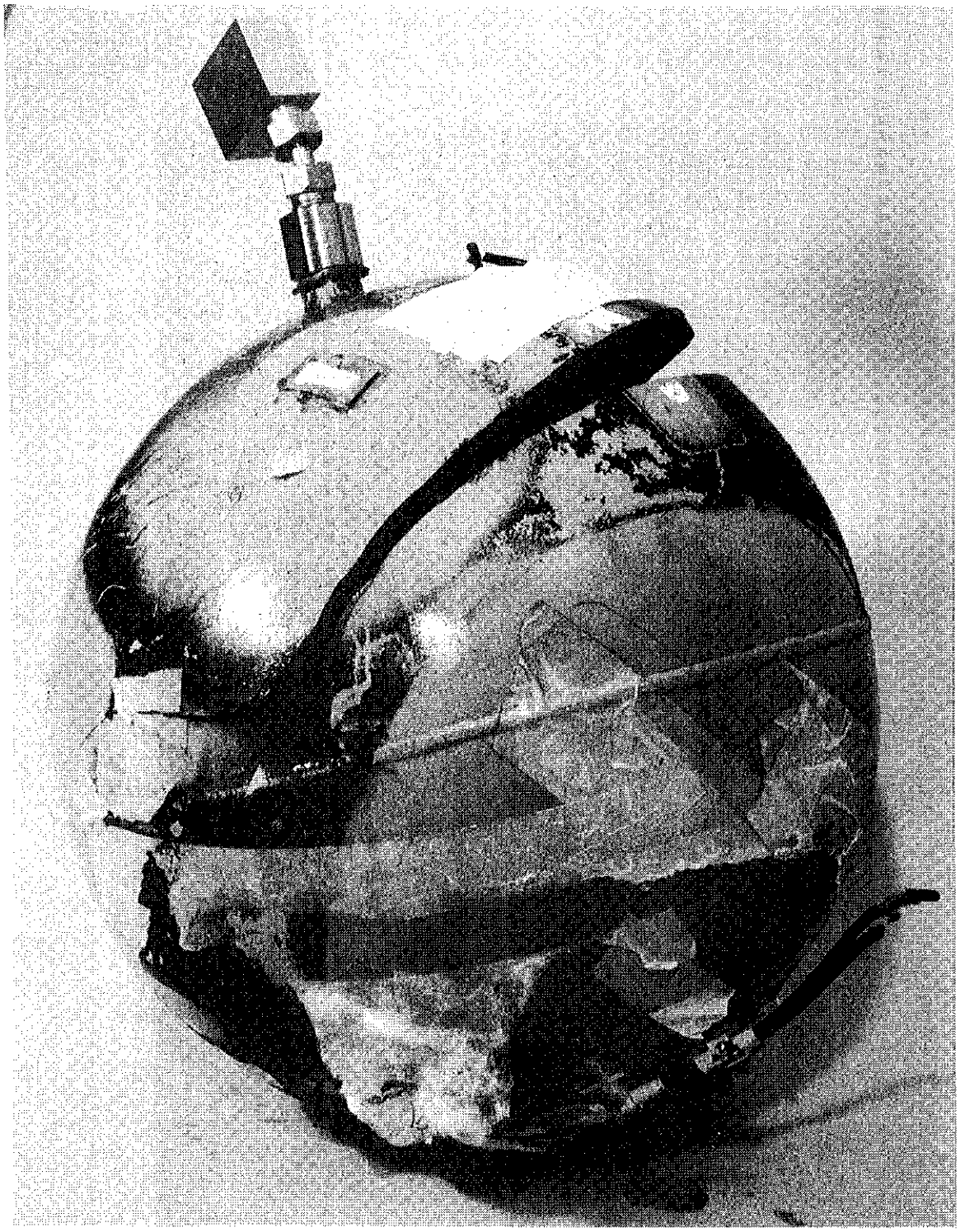

FIGURE 5. BOTTLE 2 AFTER PRESSURISATION TO FAILURE

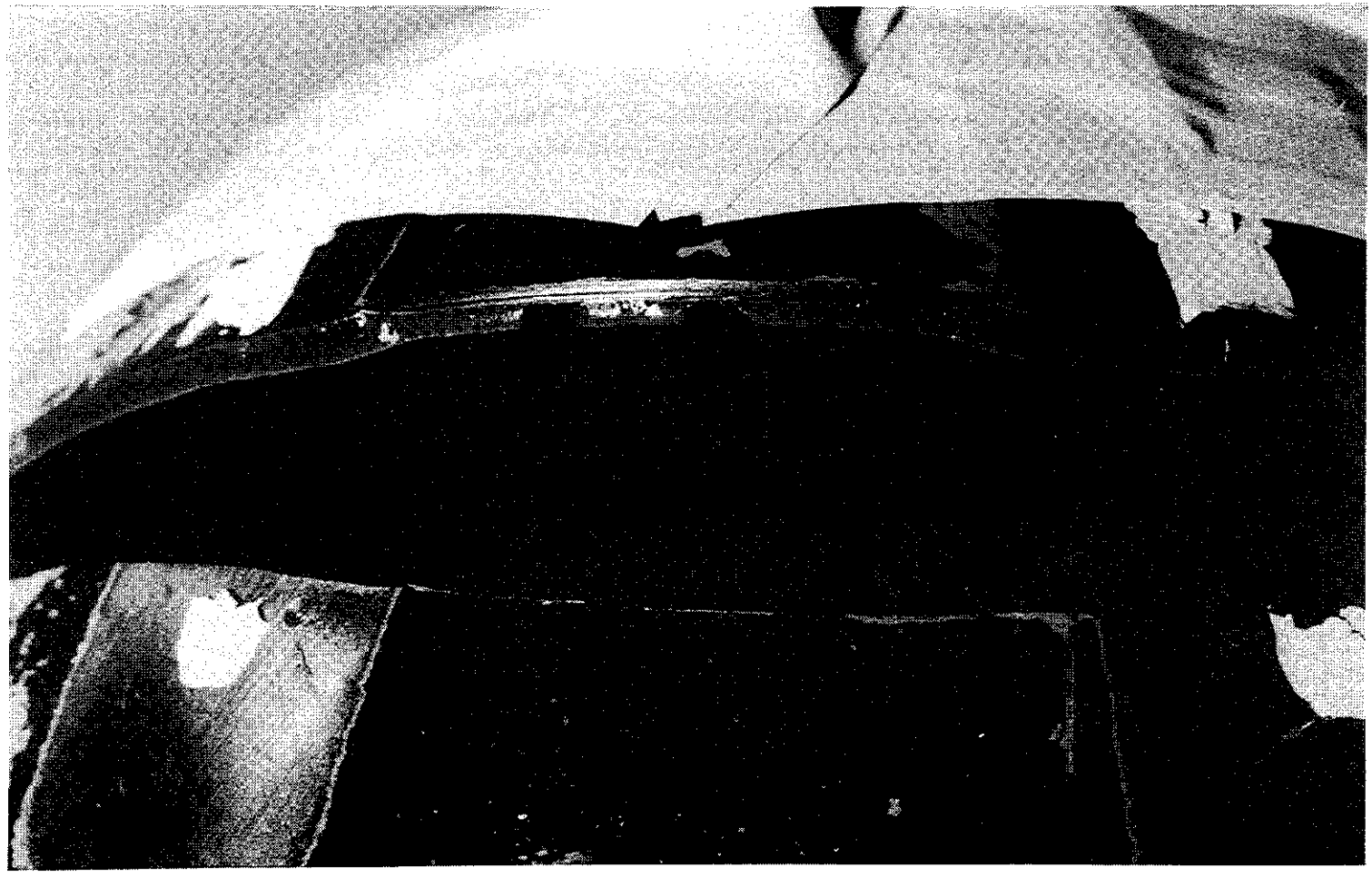

FIGURE 6. DETAIL OF THE ARTIFICIAL FLAW IN BOTTLE 2

(a)

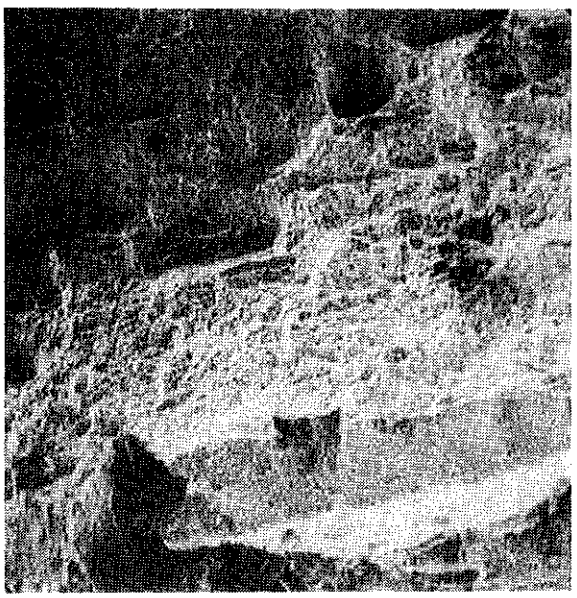

× 100

(b)

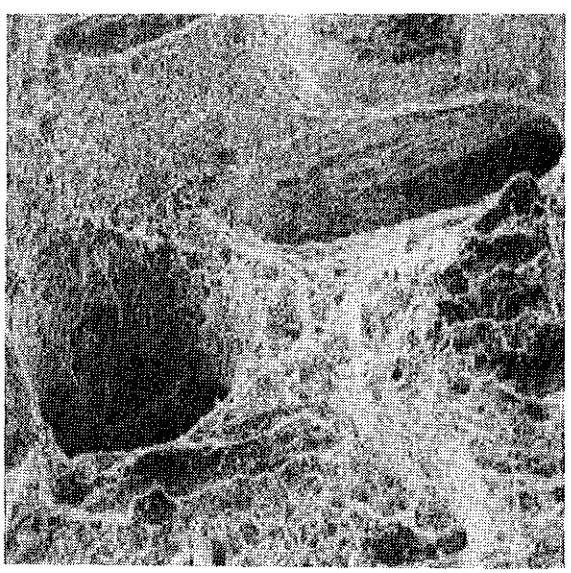

× 300

FIGURE 7. SCANNING ELECTRON MICROSCOPE PHOTOGRAPHS OF A TYPICAL SECTION OF THE FRACTURE FACE OF BOTTLE 1 (Areas of delamination parallel to the bottle surface can be seen in (b))

APPENDIX A
STRAIN GAUGE OUTPUT

In this Appendix are shown graphically the outputs of the strain gauges attached to the air bottles. Figure A1 indicates the behaviour of a gauge on bottle 1 and Figures A2 to A4 indicate that of gauges on bottle 2. The calibration of the pressure transducer and pressure gauge is shown in Figures A5 and A6 respectively.

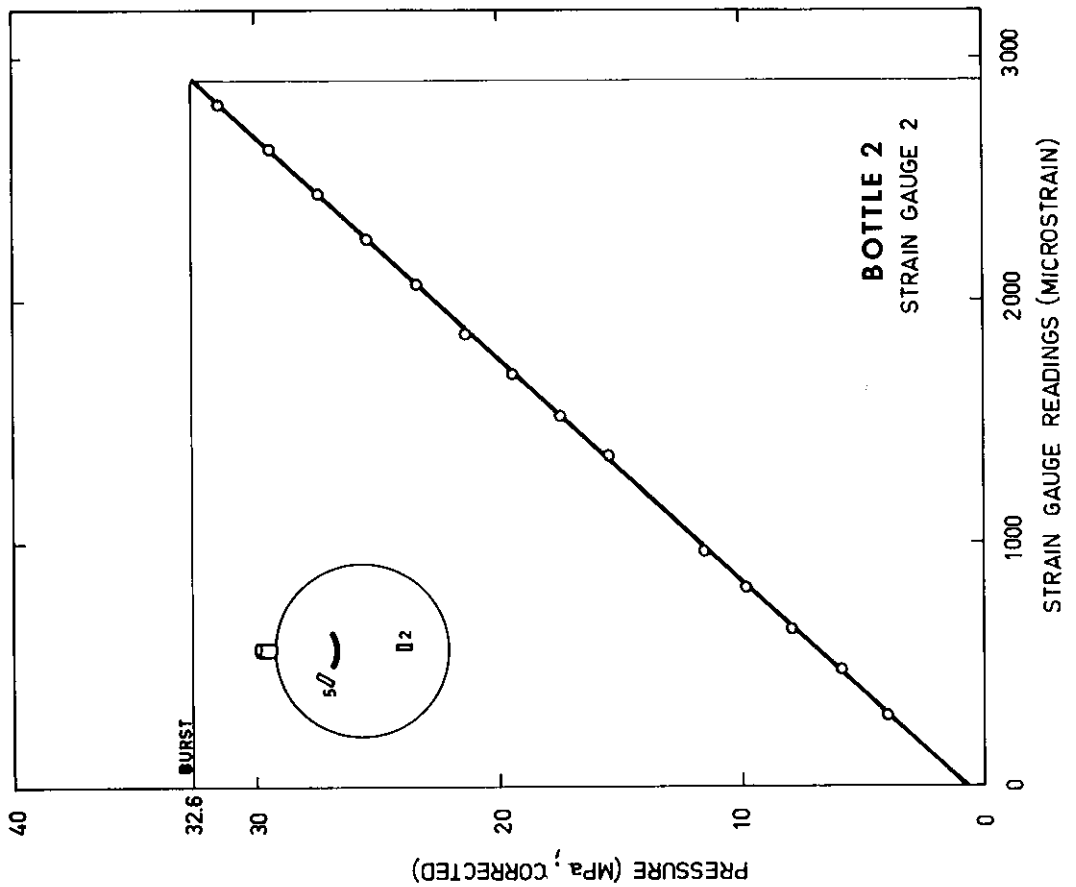

FIGURE A2. PLOT OF STRAIN AGAINST INTERNAL PRESSURE FOR BOTTLE 2

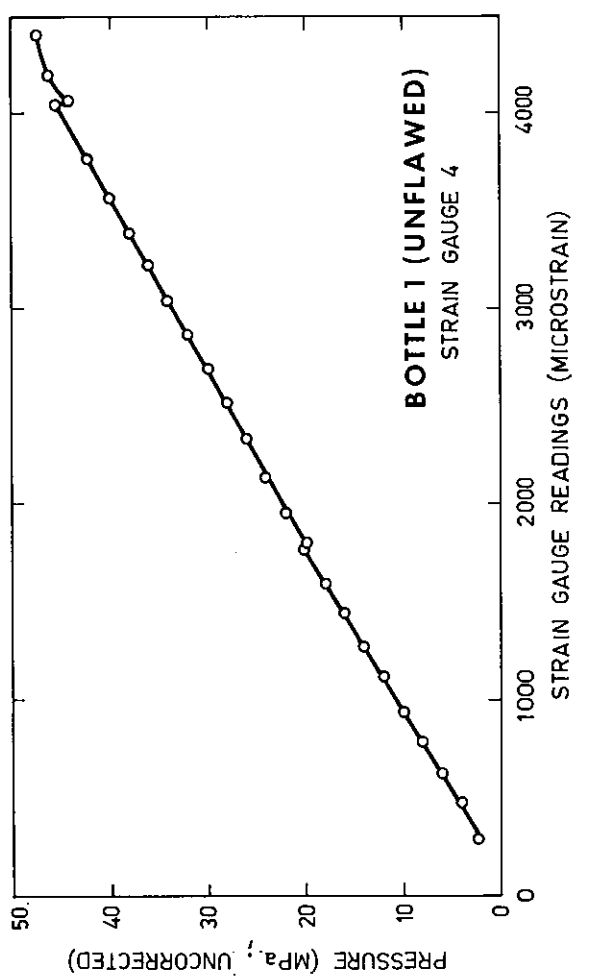

FIGURE A1. PLOT OF STRAIN AGAINST INTERNAL PRESSURE FOR BOTTLE 1

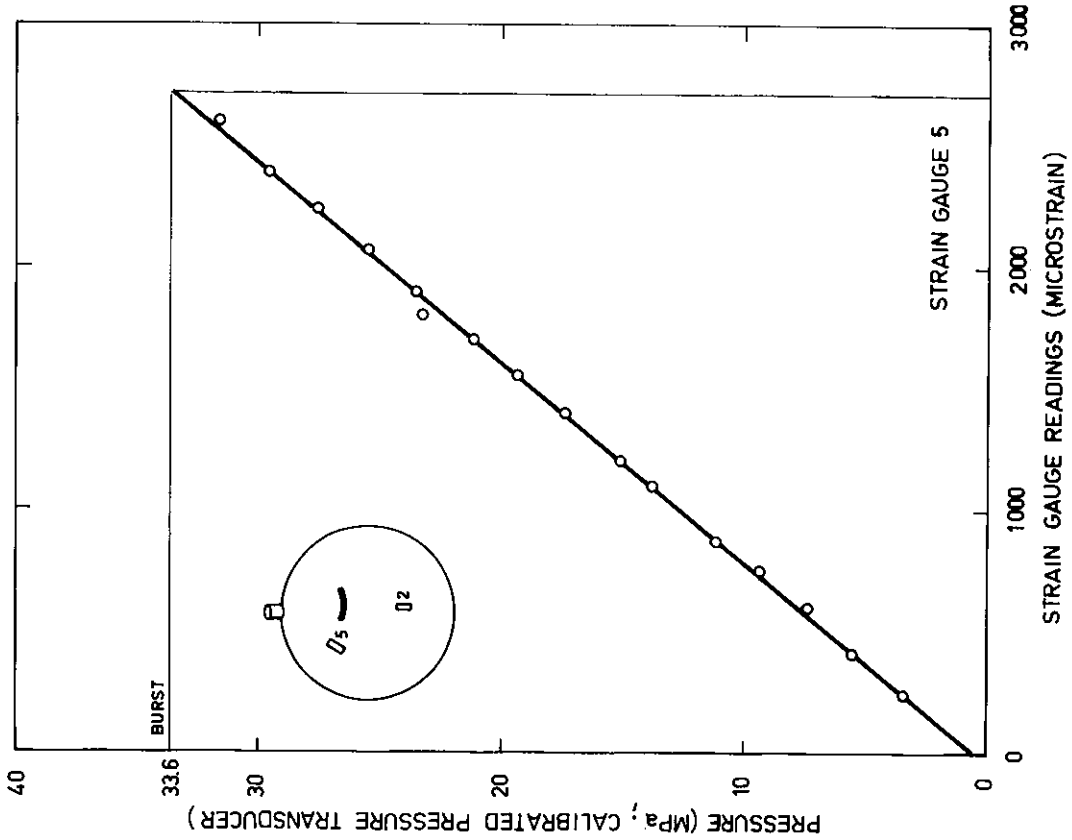

FIGURE A3. PLOT OF STRAIN AGAINST INTERNAL PRESSURE FOR BOTTLE 2

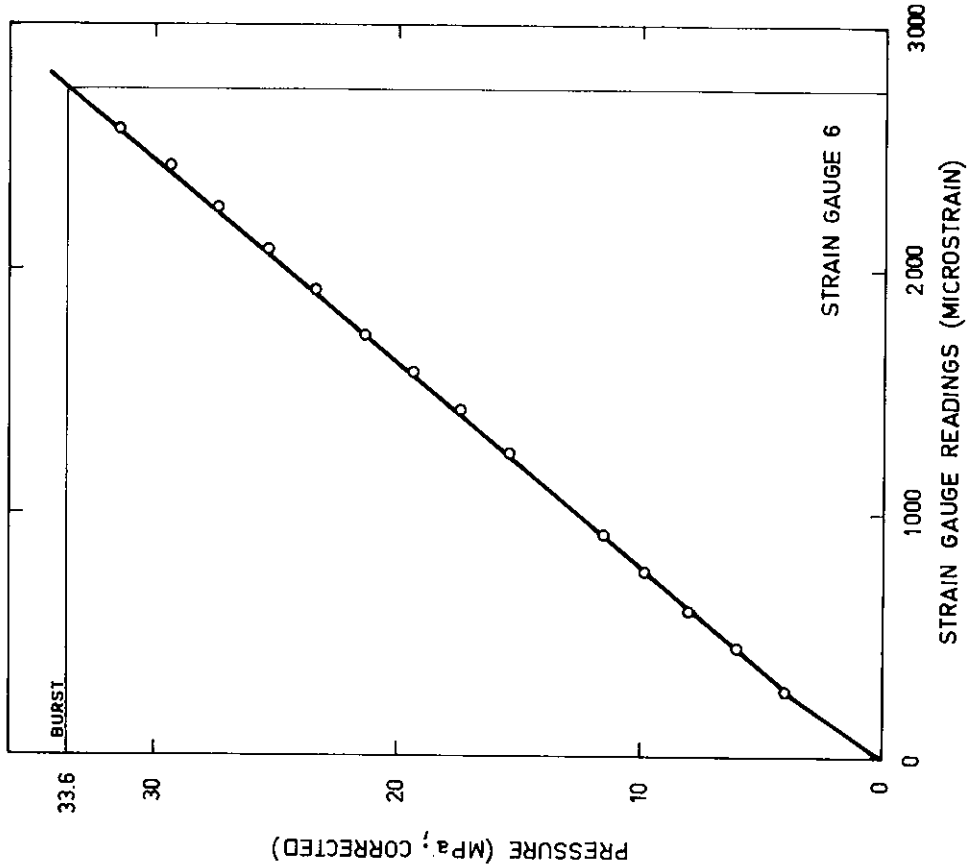

FIGURE A4. PLOT OF STRAIN AGAINST INTERNAL PRESSURE FOR BOTTLE 2

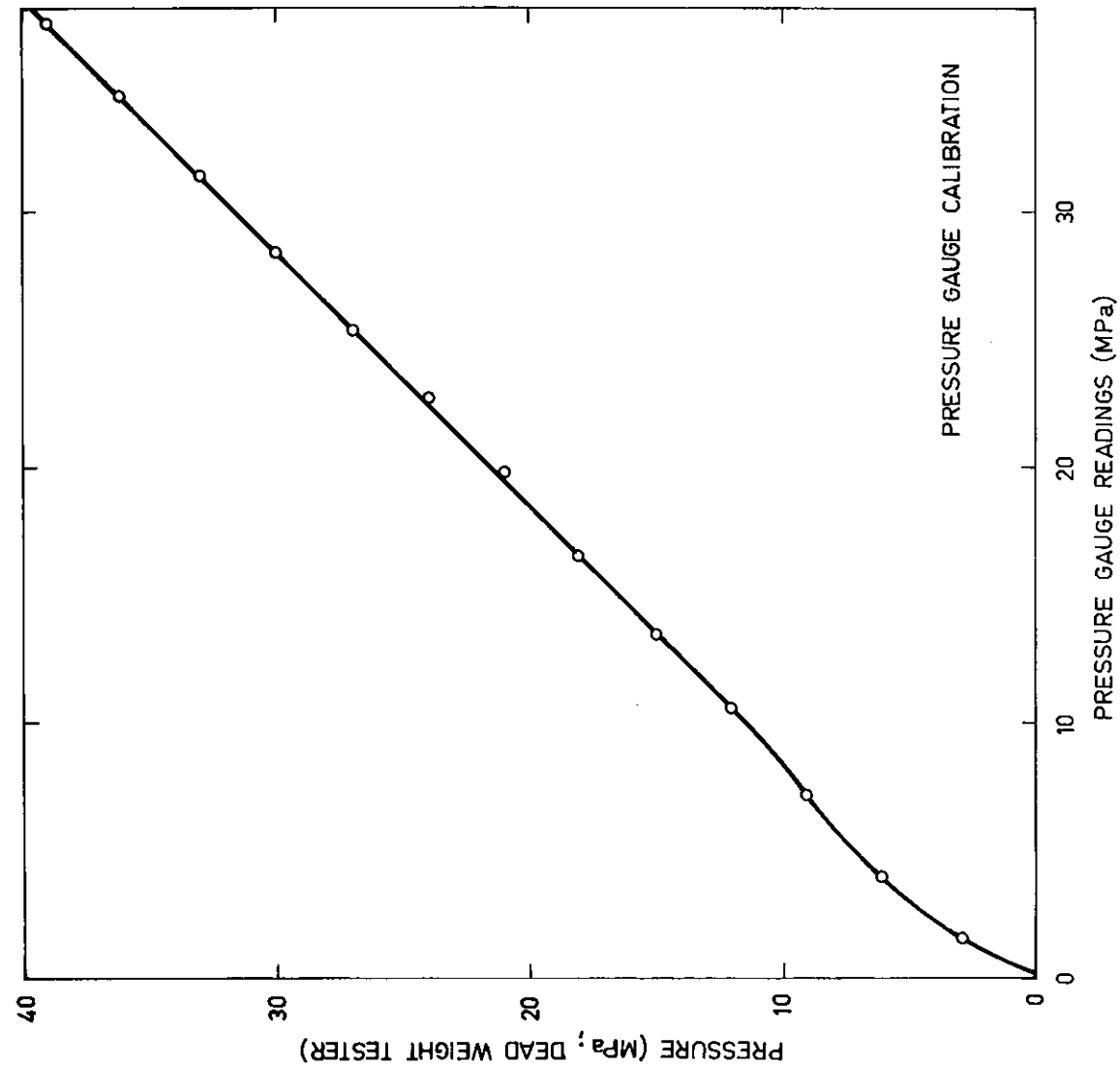

FIGURE A6. CALIBRATION OF PRESSURE GAUGE AGAINST A DEAD WEIGHT TESTER

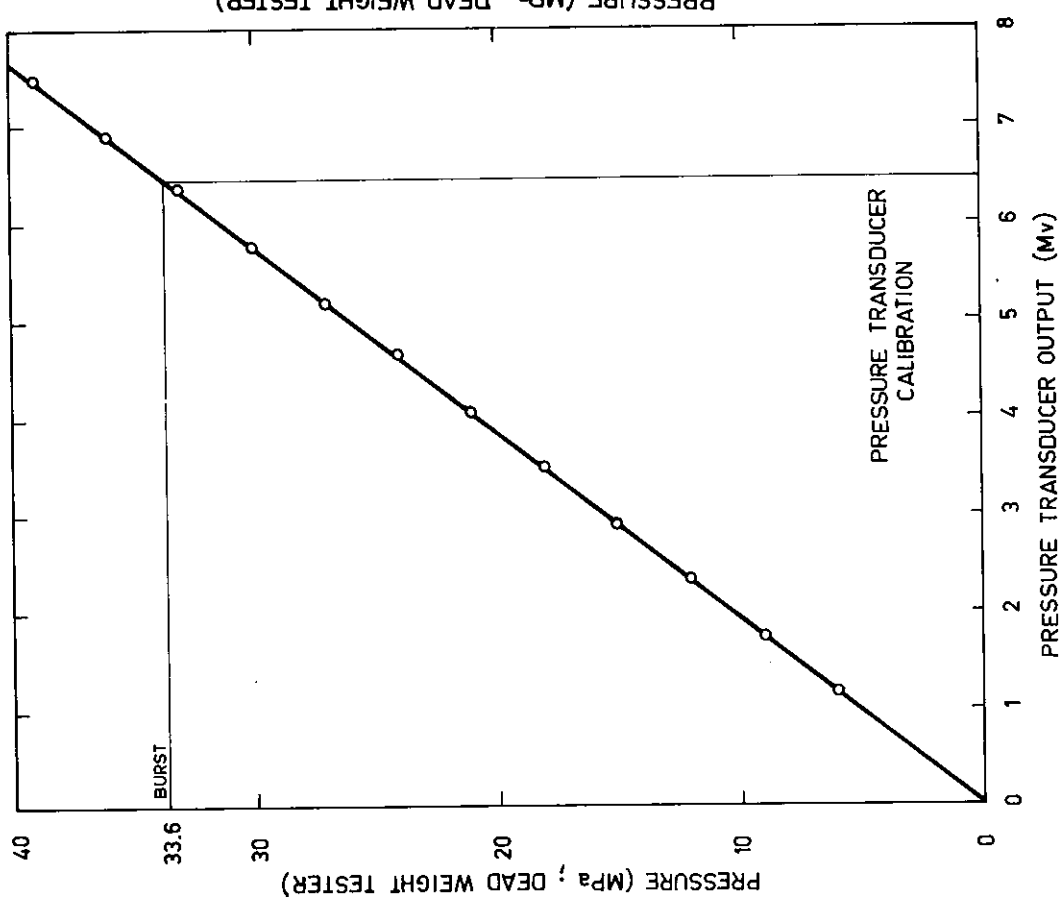

FIGURE A5. CALIBRATION OF PRESSURE TRANSDUCER AGAINST A DEAD WEIGHT TESTER